

Inelastic transport in the Coulomb blockade regime within a nonequilibrium atomic limit

Michael Galperin,^{1,*} Abraham Nitzan,² and Mark A. Ratner³

¹*Department of Chemistry and Biochemistry, University of California San Diego, La Jolla, California 92093-0340, USA*

²*School of Chemistry, The Sackler Faculty of Sciences, Tel Aviv University, Tel Aviv 69978, Israel*

³*Department of Chemistry and Materials Research Center, Northwestern University, Evanston, Illinois 60208, USA*

(Received 12 June 2008; published 18 September 2008)

A method developed by Sandalov *et al.* [Int. J. Quantum Chem. **94**, 113 (2003)] is applied to inelastic transport in the case of strong correlations on the molecule, which is relatively weakly coupled to contacts. The ability of the approach to deal with the transport in the language of many-body molecular states as well as to take into account charge-specific normal modes and nonadiabatic couplings is stressed. We demonstrate the capabilities of the technique within simple model calculations and compare it to previously published approaches.

DOI: 10.1103/PhysRevB.78.125320

PACS number(s): 73.23.-b, 85.65.+h, 71.38.-k, 73.63.Kv

I. INTRODUCTION

The development of experimental capabilities dealing with nanostructures brings the necessity of having an appropriate theoretical description of quantum transport (charge, spin, and heat) in mesoscopic junctions to the forefront of research.¹ Indeed, a lot of work has been done in this direction. In particular, many approaches are based on the Landauer expression for current through such junctions in the elastic tunneling regime.² One of the specific features of molecular transport junctions, the focus of molecular electronics, is the flexibility of the molecules, which results in inelastic features being much more pronounced in transport through such junctions as compared, e.g., to semiconductor quantum dots. Inelastic features are used as a diagnostic tool, helping to ensure the presence of the molecule and study its characteristics in the junction within inelastic electron tunneling spectroscopy in both the off-resonant (IETS) (Ref. 3) and the resonant (RIETS) (Ref. 4) situations. Detailed discussion of the inelastic transport in molecular junctions can be found in Refs. 5 and 6.

Theoretical description of IETS is well established today within both simple models^{7–12} and more realistic calculations.^{13–18} The ability to predict quantitatively experimental findings is a sign of the maturity of the field. From theoretical perspective this success is caused by the ability to use the well-established nonequilibrium perturbation (in electron-vibration coupling) technique. Indeed, in the off-resonant situation the electron-vibration coupling M is an effectively small parameter, $M \ll \sqrt{\Delta E^2 + (\Gamma/2)^2}$, with ΔE being resonant offset and Γ characterizing the strength of molecule-contact coupling. This allows expansion of the evolution operator in powers of M ; truncation at low (M^2) order, the Born approximation, is usually sufficient to get quantitatively correct predictions of IETS signal in molecular junctions.

The resonant tunneling situation, $\Delta E=0$, provides richer physics. While weak electron-vibration coupling, $M \ll \Gamma$, is also treated within perturbation theory here,^{19,20} the latter fails in the opposite situation, $M > \Gamma$, where, e.g., formation of polaron on the molecule becomes possible. Theoretically this case until now has been mostly treated either within

scattering theory (or isolated molecule) approach^{21–24} or within quasiclassical (rate or generalized rate equation) scheme.^{20,25,26} While the first treats electron-vibrational interaction (numerically) exactly, it disregards Fermi populations in the contacts, as well as dynamical features due to their presence,²⁷ and may lead to erroneous predictions.^{20,28} The latter disregards quantum correlations and as such is applicable to either high-temperature, $k_B T \gg \hbar \omega$ (truly classical) situations or (for generalized rate equation approach) quantum situations where correlations in the system die much quicker than electron transfer (between contact and molecule) time ($\sim 1/\Gamma$). Moreover, these schemes lack a formal procedure for improvement of their results similar to taking into account higher-order terms in perturbative expansion. Recently we proposed a nonequilibrium equation-of-motion (EOM) approach perturbative in molecule-contact coupling that is capable of dealing with the RIETS situation.²⁸ The approach is formulated for a simple resonant level model, but can be easily generalized for more realistic situations.²⁹ While it incorporates contacts (and hence the nonequilibrium character of the junction) into consideration, the price to pay is (generally) a more approximate level of description of electron-vibration interaction on the bridge. Alternatively, schemes exploring particular parameter regions [slow vibration $\omega_0 < \Gamma$ (Refs. 30–32) and small, $V \ll \omega_0$,³³ or big, $V \gg \omega_0$,³⁴ bias] were proposed at the model level.

Another point especially important for resonant transport (both elastic and inelastic), where actual oxidation or reduction of the molecule takes place, is the necessity to speak in the language of many-body molecular states contrary to single-particle molecular orbitals (the latter is used in most *ab initio* transport calculations today). This includes electronic structure reorganization upon charging, state dependent vibrational modes, anharmonicities, and non-Born-Oppenheimer couplings. First schemes trying to treat transport in a many-body molecular state language were recently proposed.^{25,26,35}

Difficulties in describing RIETS stem from the absence of a well-established *nonequilibrium atomic limit* for the molecule in the junction. Indeed, contacts play the role of boundary conditions responsible for establishing a nonequilibrium state of the molecule. The latter is a complicated mixture of different charge (and excitation) states. The approaches de-

veloped in the molecular electronics community so far either disregard boundary conditions and treat the molecule as an equilibrium object (scattering theory and isolated molecule treatments) or establish this nonequilibrium state [mostly nonequilibrium Green's function (NEGF) approaches], being unable to map it into separate charge (or more exactly state) constituents. Note that density-matrix-based schemes capable of such mapping were developed recently.^{36,37} Such schemes, however, miss time correlations, which may become important in, e.g., noise spectrum calculations.

The Hubbard operators are a natural language used to talk about a system (in our case, the subsystem is the molecule) in terms of its states. Thus one seems to be interested in utilizing the nonequilibrium Hubbard operator Green's function technique for description of situations similar to RIETS, where the ability to establish a nonequilibrium atomic limit of the system is desirable. The approach should be capable of providing a systematic way of taking correlations into account (similar to perturbative expansion in standard diagrammatic techniques). Such approach, originating from Kadanoff and Baym's functional derivative EOM scheme, was developed in the form of equilibrium Hubbard operator Green's functions (GFs) by Sandalov *et al.*³⁸ for materials with strong electron correlations (magnets with localized and partly localized moments, Mott insulators, Kondo lattices, heavy fermion systems, and high- T_c superconductors). The method so far has been applied in modeling elastic transport through quantum dots³⁹⁻⁴¹ and the lowest states of double quantum dots,⁴²⁻⁴⁵ and is completely ignored in the molecular electronics community.

The goals of our present consideration are to introduce inelastic transport description in the Coulomb blockade regime within a proper nonequilibrium atomic limit, and to attract the attention of the molecular electronics community to the proper nonequilibrium approach that is capable of speaking in the language of many-particle states (rather than single-particle orbitals) and that takes into account both molecular charge state dependent normal modes (presently largely ignored in simulations) and nonadiabatic couplings. Note that the Kondo physics is beyond the scope of current consideration. The approach takes into account only on-the-molecule correlations in a way that generalizes previous considerations.^{25,26} Note also that including many-body molecular states into consideration of transport potentially allows for:

(1) much more accurate molecular structure simulation out of equilibrium than in current *ab initio* schemes, due to the possibility of employing equilibrium quantum chemistry methods as a starting point for a self-consistent procedure;

(2) proper treatment of oxidation/reduction and corresponding electronic and vibrational molecular structure changes, as well as nonadiabatic couplings;

(3) the ability to deal with a general form of electron-vibration interaction as long as it is localized in space (in the spirit of Ref. 23 but in addition retaining the many-body character of the junction);

(4) calculation of noise spectrum of the junction due to preserved time correlations (see, e.g., Ref. 46 for detailed discussion); and

(5) proper treatment of degenerate situations due to preserved space correlations (see, e.g., Ref. 47 for discussion).

The structure of the paper is as follows: In Sec. II we briefly describe the method in terms of many-body states of the system, and compare it to the previously proposed generalized master-equation scheme. Section III presents numerical examples of its application to transport with discussion. Section IV concludes.

II. METHOD

Here we introduce the model of the molecular junction, briefly review the basics of the nonequilibrium Hubbard Green's function technique, and compare it to the previously proposed generalized master-equation approach.

A. Model

As usual we consider a molecular junction consisting of three parts: the left (L) and right (R) contacts and the molecule (M). The contacts are assumed to be reservoirs of free electrons each at its own equilibrium. The molecule (or the supermolecule if inclusion of parts of contacts is required) is the nonequilibrium part of the system. In addition, any external potential, e.g., gate voltage probe, or additional contacts can be added to the picture if necessary. The Hamiltonian of the system is

$$\hat{H} = \hat{H}_L + \hat{H}_M + \hat{H}_R + \hat{H}_T, \quad (1)$$

where \hat{H}_K ($K=L, R$) is the Hamiltonian for contact K ,

$$\hat{H}_K = \sum_{k \in K} \varepsilon_k \hat{c}_k^\dagger \hat{c}_k, \quad (2)$$

\hat{H}_M is the Hamiltonian of the isolated molecule, and \hat{H}_T is the coupling between the subsystems,

$$\hat{H}_T = \sum_{k \in \{L, R\}; m \in M} (V_{km} \hat{c}_k^\dagger \hat{a}_m + V_{mk} \hat{a}_m^\dagger \hat{c}_k). \quad (3)$$

\hat{a}^\dagger (\hat{a}) and \hat{c}^\dagger (\hat{c}) are creation (annihilation) operators for electrons on the molecule and in the contacts, respectively. Their indices m and k denote the electronic state in some chosen single-particle basis, and incorporate all the necessary quantum indices (e.g., site and spin).

Now we want to consider the molecular subsystem on the basis of *many-body states* $|N, i\rangle$, where N stands for molecular charge (number of electrons or excess electrons on the molecule) and i numerates different (e.g., excitation) states within the same charge state block. Generally these states should not be orthonormal, and consequences of overlap between different molecular states (as well as overlap of molecular and contact states) were considered in several papers.^{38,48} In what follows however we chose the states $|N, i\rangle$ to be orthonormal,

$$\langle N, i | N', i' \rangle = \delta_{N, N'} \delta_{i, i'}, \quad (4)$$

in order to keep the notation as simple as possible. The Hubbard operators are introduced as usual,

$$\hat{X}_{(N, i; N', i')} \equiv |N, i\rangle \langle N', i'|. \quad (5)$$

In terms of these many-body states the transfer Hamiltonian becomes

$$\hat{H}_T = \sum_{k \in \{L,R\}; \mathcal{M}} (V_{k\mathcal{M}} \hat{c}_k^\dagger \hat{X}_{\mathcal{M}} + V_{\overline{\mathcal{M}}k} \hat{X}_{\mathcal{M}}^\dagger \hat{c}_k), \quad (6)$$

where

$$\mathcal{M} \equiv (N, i; N+1, j) \quad (7)$$

denotes the transition of the system from state $|N+1, j\rangle$ to state $|N, i\rangle$, while $\overline{\mathcal{M}} \equiv (N+1, j; N, i)$ stands for the backward transition. The transfer-matrix element is

$$V_{k\mathcal{M}} \equiv \sum_{m \in \mathcal{M}} V_{km} \langle N, i | \hat{d}_m | N+1, j \rangle \quad (8)$$

and $V_{\overline{\mathcal{M}}k} = V_{k\mathcal{M}}^*$. Often many-body states are chosen as the eigenstates of isolated molecule; in this case

$$\hat{H}_{\mathcal{M}} = \sum_{|N,i\rangle} E_{N,i} \hat{X}_{(N,i;N,i)}, \quad (9)$$

with $E_{N,i}$ as the energies of the isolated molecular states.

B. Current expression

Following derivation by Meir and Wingreen,^{49,50} one gets the usual expression for the current at interface $K=L, R$,

$$I_K(t) = \frac{e}{\hbar} \int_{-\infty}^t dt_1 \text{Tr}[\Sigma_K^<(t, t_1) G^>(t_1, t) + G^>(t, t_1) \Sigma_K^<(t_1, t) - \Sigma_K^>(t, t_1) G^<(t_1, t) - G^<(t, t_1) \Sigma_K^>(t_1, t)], \quad (10)$$

which for the steady-state situation simplifies to

$$I_K = \frac{e}{\hbar} \int_{-\infty}^{+\infty} \frac{dE}{2\pi} \text{Tr}[\Sigma_K^<(E) G^>(E) - \Sigma_K^>(E) G^<(E)]. \quad (11)$$

The only difference from the standard NEGF expression is that $\text{Tr}[\dots]$ in Eqs. (10) and (11) goes not over single-electron basis but over the basis of *single-electron transitions* \mathcal{M} , Eq. (7), between the many-particle states of the molecule.

The self-energies Σ_K in Eqs. (10) and (11) are defined on the Keldysh contour as

$$[\Sigma_K(\tau, \tau')]_{\mathcal{M}\mathcal{M}'} \equiv \sum_{k \in K} V_{\overline{\mathcal{M}}k} g_k(\tau, \tau') V_{k\mathcal{M}'}, \quad (12)$$

with

$$g_k(\tau, \tau') \equiv -i \langle T_c \hat{c}_k(\tau) \hat{c}_k^\dagger(\tau') \rangle \quad (13)$$

as the GF for free electrons in the contacts. The self-energies' (SEs') projections are

$$[\Sigma_K^<(E)]_{\mathcal{M}\mathcal{M}'} = i \Gamma_{\mathcal{M}\mathcal{M}'}^K(E) f_K(E), \quad (14)$$

$$[\Sigma_K^>(E)]_{\mathcal{M}\mathcal{M}'} = -i \Gamma_{\mathcal{M}\mathcal{M}'}^K(E) [1 - f_K(E)], \quad (15)$$

where

$$\Gamma_{\mathcal{M}\mathcal{M}'}^K(E) \equiv \sum_{k \in K} V_{\overline{\mathcal{M}}k} V_{k\mathcal{M}'} \delta(E - \varepsilon_k) \quad (16)$$

and $f_K(E)$ is the Fermi distribution in contact K .

The GFs in Eqs. (10) and (11) are the Hubbard operator GFs defined on the Keldysh contour as

$$G_{\mathcal{M}\mathcal{M}'}(\tau, \tau') \equiv -i \langle T_c \hat{X}_{\mathcal{M}}(\tau) \hat{X}_{\mathcal{M}'}^\dagger(\tau') \rangle. \quad (17)$$

Note that the operators in Eqs. (13) and (17) are in the Heisenberg representation. Note also that \mathcal{M} and \mathcal{M}' in Eq. (17) may be (in principle) arbitrarily far away from one another in the charge space. GF (17) represents the correlation between different single-electron molecular many-body state transitions due to coupling to the same bath (contacts). In practice, however, it seems unreasonable to go beyond correlations between nearest charge space blocks.

In order to show the connection of the present formalism to the previously proposed generalized rate equation (master equation in the Fock space) approach, we have to realize that the latter misses correlations in both space and time. So to reduce the present GF description to the master equation in the Fock space, we need to make several simplifications:

(1) *Diagonal approximation.* We have to stick to diagonal elements of GFs only, $G_{\mathcal{M}\mathcal{M}}$ with $\mathcal{M}=(N, i; N+1, j)$.

(2) *Markov approximation.* We have to consider only GFs of equal times, $G(t, t)$. In order to reduce GFs of different times entering Eq. (11) to equal-time quantities, we use the approximation

$$G_{\mathcal{M}\mathcal{M}}(t-t') \approx \exp[i\Delta_{\mathcal{M}}^0(t'-t)] G_{\mathcal{M}\mathcal{M}}(t-t), \quad (18)$$

where

$$\Delta_{\mathcal{M}}^0 \equiv E_{N+1,j} - E_{N,i}. \quad (19)$$

Now, noting that

$$iG_{\mathcal{M}\mathcal{M}}^>(t-t) = P_i^N, \quad (20)$$

$$-iG_{\mathcal{M}\mathcal{M}}^<(t-t) = P_j^{N+1} \quad (21)$$

are the probabilities of finding the molecule in states $|N, i\rangle$ and $|N+1, j\rangle$, respectively, we get from Eq. (11)

$$I_K = \frac{e}{\hbar} \sum_{N,i,j} \{ \Gamma_{(N,i;N+1,j)}^K f_K(E_j^{N+1} - E_i^N) P_i^N - \Gamma_{(N,i;N+1,j)}^K [1 - f_K(E_j^{N+1} - E_i^N)] P_j^{N+1} \}. \quad (22)$$

If now we restrict our attention only to particular charge space block N_0 and its nearest neighbors, we get Eqs. (6) and (7) of Ref. 25.

C. General equation for GF

Now, after the expression for the current has been established, we need a procedure to calculate the Hubbard operators' GF [Eq. (17)]. Note that standard diagrammatic techniques are inapplicable here, due to the absence of the Wick theorem (since Hubbard operators are many-particle operators). An alternative to diagrammatic expansion in the form of functional derivative equation-of-motion technique was developed in Ref. 38. Here we briefly review the steps needed to obtain the EOM for GF, which we will use in our numerical simulations.

Following Ref. 38, we start by writing the EOM for the Hubbard operator $\hat{X}_{\mathcal{M}}(\tau)$, where $\mathcal{M} \equiv (N, i; N+1, j)$. This leads to

$$\begin{aligned} & \left[i \frac{\partial}{\partial \tau} - \Delta_{\mathcal{M}}^0 \right] \hat{X}_{\mathcal{M}}(\tau) \\ &= \sum_{k \in \{L, R\}; \ell} [-V_{k(N+1, j; N+2, \ell)} \hat{c}_k^\dagger(\tau) \hat{X}_{(N, i; N+2, \ell)}(\tau) \\ & \quad - V_{k(N-1, \ell; N, i)} \hat{c}_k^\dagger(\tau) \hat{X}_{(N-1, \ell; N+1, j)}(\tau) \\ & \quad + V_{(N+1, j; N, \ell)k} \hat{X}_{(N, i; N, \ell)}(\tau) \hat{c}_k(\tau) \\ & \quad + V_{(N+1, \ell; N, i)k} \hat{X}_{(N+1, \ell; N+1, j)}(\tau) \hat{c}_k(\tau)]. \end{aligned} \quad (23)$$

In what follows we disregard the first two terms on the right-hand side, since they describe simultaneous transfer of two electrons between contact and molecule, which is beyond the scope of the present consideration. It is clear that when writing the EOM for GF (17), the terms on the right-hand side of Eq. (23) will produce correlation functions of the form

$$\langle T_c \hat{X}_{\xi}(\tau) \hat{c}_k(\tau) \hat{X}_{\mathcal{M}'}^\dagger(\tau') \rangle, \quad (24)$$

which cannot be factorized into the product of single-excitation GF [Eq. (17)] and contact single-electron GF [Eq. (13)] due to the absence of the Wick theorem.

In order to make this separation, a trick with auxiliary fields $\mathcal{U}_{\xi}(\tau)$ is employed. We need to introduce the additional disturbance potential

$$\hat{H}_{\mathcal{U}}(\tau) \equiv \sum_{N, i, j} \mathcal{U}_{(N, i; N, j)}(\tau) \hat{X}_{(N, i; N, j)}(\tau) \quad (25)$$

and the corresponding generating functional

$$\hat{S}_{\mathcal{U}} \equiv \exp \left[-i \int_c d\tau \hat{H}_{\mathcal{U}}(\tau) \right]. \quad (26)$$

Then by defining the GF of two arbitrary operators \hat{A} and \hat{B} in the presence of auxiliary fields \mathcal{U} as

$$G_{AB}(\tau, \tau') \equiv -i \langle T_c \hat{A}(\tau) \hat{B}(\tau') \rangle_{\mathcal{U}} \equiv -i \frac{\langle T_c \hat{S}_{\mathcal{U}} \hat{A}(\tau) \hat{B}(\tau') \rangle}{\langle T_c \hat{S}_{\mathcal{U}} \rangle}, \quad (27)$$

one easily can get the following identity:

$$\begin{aligned} & -i \langle T_c \hat{X}_{\xi}(\tau') \hat{A}(\tau) \hat{B}(\tau') \rangle_{\mathcal{U}} \\ &= \left[\langle T_c \hat{X}_{\xi}(\tau') \rangle_{\mathcal{U}} + i \frac{\delta}{\delta \mathcal{U}_{\xi}(\tau')} \right] G_{AB}(\tau, \tau'). \end{aligned} \quad (28)$$

Equation (28) allows one to express correlation function (24) in terms of single-excitation GF and its functional derivatives relative to auxiliary fields. Note that setting (at the end) auxiliary fields to zero turns Eq. (27) into a standard definition of GF.

So when introducing auxiliary fields as in Eqs. (25) and (26) and using expression (28), one gets a general EOM for the Hubbard operator GF [Eq. (17)] in the form

$$\begin{aligned} & \left[i \frac{\partial}{\partial \tau} - \Delta_{\mathcal{M}}^0 \right] G_{\mathcal{M}\mathcal{M}'}(\tau, \tau') - \sum_{\ell} [\mathcal{U}_{(N+1, j; N+1, \ell)}(\tau) \\ & \quad \times G_{(N, i; N+1, \ell)\mathcal{M}'}(\tau, \tau') - \mathcal{U}_{(N, \ell; N, i)}(\tau) G_{(N, \ell; N+1, j)}(\tau, \tau')] \\ &= \delta(\tau, \tau') P_{\mathcal{M}\mathcal{M}'}(\tau) \\ & \quad + \sum_{\ell} \left\{ \left[\langle T_c \hat{X}_{(N, i; N, \ell)}(\tau) \rangle_{\mathcal{U}} + i \frac{\delta}{\delta \mathcal{U}_{(N, i; N, \ell)}(\tau)} \right] \right. \\ & \quad \times \sum_{\mathcal{M}''} \int_c d\tau'' \Sigma_{(N, \ell; N+1, j)\mathcal{M}''}(\tau, \tau'') G_{\mathcal{M}''\mathcal{M}'}(\tau'', \tau') \\ & \quad + \left[\langle T_c \hat{X}_{(N+1, \ell; N+1, j)}(\tau) \rangle_{\mathcal{U}} + i \frac{\delta}{\delta \mathcal{U}_{(N+1, \ell; N+1, j)}(\tau)} \right] \\ & \quad \left. \times \sum_{\mathcal{M}''} \int_c d\tau'' \Sigma_{(N, i; N+1, \ell)\mathcal{M}''}(\tau, \tau'') G_{\mathcal{M}''\mathcal{M}'}(\tau'', \tau') \right\}, \end{aligned} \quad (29)$$

where $\Delta_{\mathcal{M}}^0$ is defined in Eq. (19) and

$$P_{\mathcal{M}\mathcal{M}'} \equiv \langle T_c \hat{X}_{(N, i; N, i')}(\tau) + \hat{X}_{(N+1, j'; N+1, j)}(\tau) \rangle_{\mathcal{U}}. \quad (30)$$

Equation (29) is a general equation for the Hubbard operator GF, representing an alternative to standard diagrammatic technique approaches. The functional derivatives in auxiliary fields play the role of expansion in small parameter. The level of approximation is defined by the order of the derivative used in the evaluation of GF. At the end of differentiations auxiliary fields are set to zero, and the resulting expression is the equation for GF at the particular level of approximation.

D. First loop approximation

The simplest approximation, Hubbard I (HI), is obtained from Eq. (29) by keeping only diagonal averages, omitting all functional derivatives, and letting $\mathcal{U} \rightarrow 0$,

$$\begin{aligned} & \left[i \frac{\partial}{\partial \tau} - \Delta_{\mathcal{M}}^0 \right] G_{\mathcal{M}\mathcal{M}'}(\tau, \tau') \\ &= \delta(\tau, \tau') \delta_{\mathcal{M}\mathcal{M}'} P_{\mathcal{M}} \\ & \quad + P_{\mathcal{M}} \sum_{\mathcal{M}''} \int_c d\tau'' \Sigma_{\mathcal{M}\mathcal{M}''}(\tau, \tau'') G_{\mathcal{M}''\mathcal{M}'}(\tau'', \tau'). \end{aligned} \quad (31)$$

Following most of the papers that employed the method so far,^{39–41} in our consideration we go one step further: We take one functional derivative to get the so-called first loop approximation. Note here that we take the derivative of GF only, disregarding fluctuations of the spectral weight P . After performing the differentiation, we keep only diagonal averages, omit all functional derivatives, and let $\mathcal{U} \rightarrow 0$. Since the procedure was described in detail in many papers (see, e.g., Refs. 38 and 41), here we present only the final result,

$$\begin{aligned}
& \left[i \frac{\partial}{\partial \tau} - \Delta_{\mathcal{M}}^0 \right] G_{\mathcal{M}, \mathcal{M}'}(\tau, \tau') - i \sum_{\kappa, \ell} \sum_{\mathcal{M}''} \int_c d\tau'' [\Sigma_{(N, \kappa; N+1, j), \mathcal{M}''}(\tau, \tau'') D_{\mathcal{M}''(N-1, \ell; N, i)}(\tau'', \tau+) G_{(N-1, \ell; N, \kappa), \mathcal{M}'}(\tau, \tau') \\
& - \Sigma_{(N, \kappa; N+1, j), \mathcal{M}''}(\tau, \tau'') D_{\mathcal{M}''(N, \kappa; N+1, \ell)}(\tau'', \tau+) G_{(N, i; N+1, \ell), \mathcal{M}'}(\tau, \tau') + \Sigma_{(N, i; N+1, \kappa), \mathcal{M}''}(\tau, \tau'') D_{\mathcal{M}''(N, \ell; N+1, \kappa)}(\tau'', \tau+) \\
& \times G_{(N, \ell; N+1, j), \mathcal{M}'}(\tau, \tau') - \Sigma_{(N, i; N+1, \kappa), \mathcal{M}''}(\tau, \tau'') D_{\mathcal{M}''(N+1, j; N+2, \ell)}(\tau'', \tau+) G_{(N+1, \kappa; N+2, \ell), \mathcal{M}'}(\tau, \tau')] \\
& = \delta(\tau, \tau') \delta_{\mathcal{M}, \mathcal{M}'} P_{\mathcal{M}} + P_{\mathcal{M}} \sum_{\mathcal{M}''} \int_c d\tau'' \Sigma_{\mathcal{M}, \mathcal{M}''}(\tau, \tau'') G_{\mathcal{M}'' \mathcal{M}'}(\tau'', \tau'), \tag{32}
\end{aligned}$$

where $\mathcal{M} \equiv (N, i; N+1, j)$ and D is the so-called full locator, which (in the first loop approximation) obeys the same equation [Eq. (32)] as GF but without spectral weight $P_{\mathcal{M}}$ multiplying the delta function on the right-hand side.

Expressions for the GFs G and D (first loop approximation) in the shorthand (matrix in both Fock-space and Keldysh-contour variables) notation can be written as

$$\hat{D}^{-1} G = P, \tag{33}$$

$$\hat{D}^{-1} D = 1, \tag{34}$$

where

$$\hat{D}^{-1} \equiv \left[i \frac{\partial}{\partial \tau} - \Delta_{\mathcal{M}} - P \Sigma \right], \tag{35}$$

$$\Delta_{\mathcal{M}} = \Delta_{\mathcal{M}}^0 + \delta \Delta_{\mathcal{M}}, \tag{36}$$

and $\delta \Delta_{\mathcal{M}}$, given by the second term on the left-hand side of Eq. (32), is responsible for shifts of transition energies in the molecule due to contact-induced correlation. One sees that Eq. (34) has the usual structure of the Dyson equation, which is obtained in standard diagrammatic expansion. The only difference is dressing of SE Σ by spectral weight P . Thus formally one can use all the standard equations, using dressed SE Σ everywhere, to get the desired projections of GF D . When D is known, G is obtained by simple matrix multiplication,

$$G = DP. \tag{37}$$

Note that the sides of matrix dressing by spectral weight P are different for Σ and G ; compare Eqs. (35) and (37). Note also that the scheme is self-consistent, since both transition energies shift $\delta \Delta$ and spectral weights P depend on GF G , while the latter depends on these quantities. In particular [$\mathcal{M} \equiv (N, i; N+1, j)$],

$$P_{\mathcal{M}} = N_{N, i} + N_{N+1, j}, \tag{38}$$

$$N_{N, i} \equiv \langle \hat{X}_{(N, i; N, i)}^{\hat{}} \rangle = i G_{\mathcal{M}, \mathcal{M}}^>(t, t) \text{ for any } j, \tag{39}$$

$$N_{N+1, j} \equiv \langle \hat{X}_{(N+1, j; N+1, j)}^{\hat{}} \rangle = -i G_{\mathcal{M}, \mathcal{M}}^<(t, t) \text{ for any } i. \tag{40}$$

Here $N_{N, i}$ and $N_{N+1, j}$ are the probabilities of finding the system in the states $|N, i\rangle$ and $|N+1, j\rangle$, respectively.

III. NUMERICAL RESULTS AND DISCUSSION

Here we present the results of simulations within first loop approximation. In order to speed up calculations, we also employed diagonal approximation.⁵¹ We consider transport through a quantum dot and a double quantum dot, discuss the obtained data, and compare these to previously published results.

A. Quantum dot

In the case of a quantum dot, the molecular Hamiltonian is

$$\hat{H}_{\mathcal{M}} = \sum_{\sigma=\{\uparrow, \downarrow\}} \varepsilon_{\sigma} \hat{n}_{\sigma} + U \hat{n}_{\uparrow} \hat{n}_{\downarrow}, \tag{41}$$

where σ indicates spin projection and $\hat{n}_{\sigma} = \hat{d}_{\sigma}^{\dagger} \hat{d}_{\sigma}$. The full Fock space of the molecular part of the system (without vibrations) consists of one empty state ($|0\rangle \equiv |0, 0\rangle$), two single-electron states ($|\uparrow\rangle \equiv |1, \uparrow\rangle$ and $|\downarrow\rangle \equiv |1, \downarrow\rangle$), and one doubly occupied state ($|2\rangle \equiv |2, 0\rangle$). Transitions between these states to be considered are spin-up electron transfers ($0\uparrow$ and $\downarrow 2$) and spin-down electron transfers ($0\downarrow$ and $\uparrow 2$). Writing Eq. (32) in the basis of these transitions, one gets the equations obtained in Ref. 40.

Figure 1 presents a conductance map for elastic transport through a quantum dot. The parameters of the calculation are $T=10$ K, $\varepsilon_{\sigma} = -0.5$ eV, $\Gamma_{\sigma}^K = 0.01$ eV ($\sigma = \uparrow, \downarrow$ and $K=L, R$), and $U=1$ eV. As usual one has areas of blockaded transport (inside part of diamonds) with a fixed population on the dot (0, 1, and 2 from right to left), and transition areas (between the diamonds) where the population on the dot is a noninteger (see, e.g., Ref. 52 for more detailed discussion).

In order to treat inelastic transport, we add to $\hat{H}_{\mathcal{M}}$ molecular vibration linearly coupled to electron(s) on the dot,

$$\omega_0 \hat{a}^{\dagger} \hat{a} + M(\hat{a} + \hat{a}^{\dagger}) \sum_{\sigma} \hat{n}_{\sigma}. \tag{42}$$

Such model is frequently used to describe inelastic transport in molecular junctions. In a sense it is similar to the Marcus

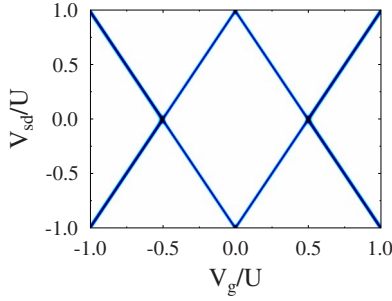


FIG. 1. (Color online) Conductance map for elastic transport through a quantum dot. See text for parameters.

theory, and it describes the shift of the molecular vibration when the molecule is charged due to electron transfer from/to the contacts. In general, the model with nondiagonal electron-vibration coupling can also be considered within the formalism.

After small polaron (Lang-Firsov or canonical) transformation,⁵³ the linear coupling term is eliminated, while the energy-level position ε_σ and the Hubbard repulsion U are renormalized ($\varepsilon_\sigma \rightarrow \varepsilon_\sigma - M^2/\omega_0$ and $U \rightarrow U - 2M^2/\omega_0$), and the transfer-matrix elements in \hat{H}_T [Eq. (3)] are dressed with shift operators ($\hat{a}_\sigma \rightarrow \hat{a}_\sigma \hat{\mathcal{X}}$)

$$\hat{\mathcal{X}} = \exp[-\lambda(\hat{a}^\dagger - \hat{a})], \quad (43)$$

where $\lambda = M/\omega_0$. In what follows we disregard the renormalization of ε_σ and U , assuming that it was included in the definition of these parameters.

Now the molecule is characterized by the direct product of electronic and vibrational spaces, so its state should be indicated by an additional index v showing the state of the vibration; i.e., the molecular subspace is spanned by the states $|0, v\rangle$, $|\uparrow, v\rangle$, $|\downarrow, v\rangle$, and $|2, v\rangle$, where $v \in \{0, 1, 2, 3, \dots\}$. One has to consider the same electronic transitions as in the case of elastic transport, but in addition all possible transitions between states of the vibration have to be included. Transitions between these states (within the model) are possible only by electron transfer between molecule and contacts. Due to shift operators [Eq. (43)] appearing in \hat{H}_T , the SEs [Eq. (12)] are now dressed with corresponding vibrational overlap integrals [$\mathcal{M} \equiv (N, i, v_i; N+1, j, v_j)$],

$$\Sigma_{\mathcal{M}, \mathcal{M}'} \rightarrow \Sigma_{\mathcal{M}, \mathcal{M}'} \times \langle v_i | \hat{\mathcal{X}} | v_j \rangle \langle v'_i | \hat{\mathcal{X}} | v'_j \rangle, \quad (44)$$

with

$$\langle v | \hat{\mathcal{X}} | v' \rangle = e^{-\lambda^2/2} (-1)^{(v-v')\theta(v-v')} \times \lambda^{v_{\max}-v_{\min}} \left[\frac{v_{\min}!}{v_{\max}!} \right]^{1/2} L_{v_{\min}}^{v_{\max}-v_{\min}}(\lambda^2), \quad (45)$$

where v_{\min} (v_{\max}) is the minimal (maximal) of v and v' , $\theta(x)$ is a step function, and L_n^m is a Laguerre polynomial. Note an important formal difference between the present approach and the one presented in Ref. 52. While in the latter we had to consider separately electron and phonon dynamics, which leads to convolution of electron GF (electron dynamics) with

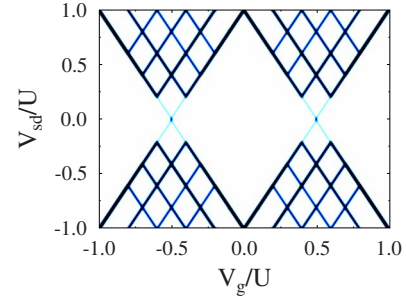


FIG. 2. (Color online) Conductance map for inelastic transport through a quantum dot. Linear coupling model (42). See text for parameters.

Franck-Condon factors (phonon dynamics), here the situation is different. Since we consider the generalized Fock space (product of electronic and vibrational ones), within the formalism strictly speaking we do not have inelastic processes at all. Instead we have to consider elastic-scattering events between electron-vibrational states. As a result the role played previously by the Franck-Condon factors (to introduce vibrational dynamics) is now included in the Hubbard GF of the generalized Fock space.

Figure 2 presents the conductance map for inelastic transport through a quantum dot within linear coupling model (42). The parameters of the calculation are $\omega_0 = 0.2$ eV and $M = 0.4$ eV; all the other parameters are as in Fig. 1. Within the calculation we restricted the vibrational subspace to the four lowest levels ($v \in \{0, 1, 2, 3\}$). As expected, besides elastic peaks in the conductance map, we get additional resonant vibrational features corresponding to inelastic processes. This figure is equivalent to Fig. 3(a) of Ref. 52, where the calculation was done within perturbative (in coupling to electrodes) nonequilibrium EOM approach for the same model. As previously,⁵² within the model (see also discussion below) the distance between the diamond edges (elastic peak) and vibrational sidebands is defined by the oscillator frequency. An increase in electron-vibrational coupling would result in both more pronounced vibrational features and suppression of transport in the low source-drain voltage region due to Franck-Condon blockade. On the other hand an increase in temperature would produce also vibrational sidebands corresponding to phonon absorption (features inside the diamond).

Finally, we want to demonstrate the capabilities of the present scheme, which go beyond those of approaches previously used to treat inelastic transport. Suppose our molecule is small enough, so that upon charging it changes its normal modes essentially. Suppose also that from all the normal modes of the molecule, only one is coupled to a tunneling electron. Inelastic transport in this case can be modeled by assigning different vibration frequencies to different charge states of the molecule. In our quantum dot model, this corresponds to the situation where the vibrational frequencies for $|0, v\rangle$, $|\sigma, v\rangle$, and $|2, v\rangle$ states are different— $\omega_0^{(0)}$, $\omega_0^{(1)}$, and $\omega_0^{(2)}$, respectively. Self-energies due to electron transfer between molecule and contacts once more have to be dressed by overlap integrals between different vibrational wave functions, as shown in Eq. (44). However this time

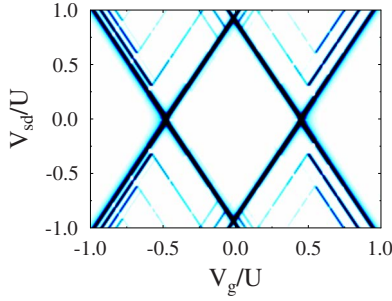


FIG. 3. (Color online) Conductance map for inelastic transport through a quantum dot. Charge state dependent frequencies. See text for parameters.

(when vibrational frequencies change), the integrals should be calculated in the way discussed in Refs. 54 and 55.

Figure 3 presents the conductance map for inelastic transport through a quantum dot, when vibrational frequency depends on charge state of the dot. The parameters of the calculation are $\omega_0^{(0)}=0.2$ eV, $\omega_0^{(1)}=0.3$ eV, and $\omega_0^{(2)}=0.25$ eV, and the shift vector for both transitions is taken to be 0.5 \AA (see Refs. 54 and 55 for detailed explanation); all the other parameters are as in Fig. 1. One sees that the result of calculation is counterintuitive at first sight. Naively one could expect to see inelastic peaks at each diamond edge (each charge state of the quantum dot) being separated by the frequency corresponding to the neighboring charge state (RIETS probes frequencies of the intermediate ion). The real picture is more complicated however. Let us consider electron transfer between two particular charge states of the quantum dot, say between states $|0, v_0\rangle$ and $|\sigma, v_1\rangle$, upon electron transfer from contact to molecule. In this case the change in the subsystem energy, which will be observed in transport as inelastic peak in conductance, is $v_1\omega_0^{(1)} - v_0\omega_0^{(0)}$. (We omit here the change in elastic electronic energy for simplicity; this will define only the position of the elastic peak in conductance.) Since v_0 and v_1 in principle can be any non-negative numbers, it is clear that one can observe a progression of frequencies. Note that in this progression one can see inelastic peaks in conductance, separated from the elastic one by a frequency which does not exist in the system at all (e.g., $\omega_0^{(1)} - \omega_0^{(0)}$). Note also that due to overlap factors involved, the lowest frequencies of the progression will be observed better in RIETS signal. Nonadiabatic couplings can be included in calculation in a similar way.

B. Double quantum dot

The molecular Hamiltonian for a double quantum dot is

$$\begin{aligned} \hat{H}_M = & \sum_{i=\{1,2\}\sigma=\{\uparrow,\downarrow\}} \varepsilon_{i\sigma} \hat{n}_{i\sigma} - t_{12,\sigma} (\hat{d}_{1\sigma}^\dagger \hat{d}_{2\sigma} + \hat{d}_{2\sigma}^\dagger \hat{d}_{1\sigma}) \\ & + \sum_i U_i \hat{n}_i \hat{n}_{i\downarrow} + U_{12} \hat{n}_1 \hat{n}_2, \end{aligned} \quad (46)$$

where $i=\{1,2\}$ numbers sites and $\sigma=\{\uparrow,\downarrow\}$ stands for spin projection, \hat{d}^\dagger (\hat{d}) is a creation (annihilation) operator, $\hat{n}_{i\sigma} = \hat{d}_{i\sigma}^\dagger \hat{d}_{i\sigma}$, and $\hat{n}_i = \hat{n}_{i\uparrow} + \hat{n}_{i\downarrow}$. We assume that site 1 is coupled to

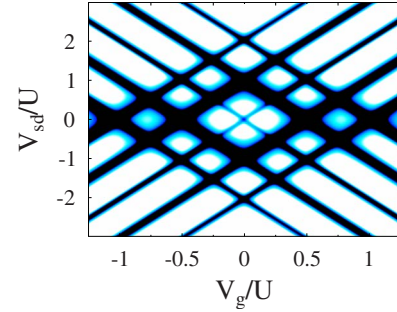


FIG. 4. (Color online) Conductance map for elastic transport through a double quantum dot. See text for parameters.

the left contact, while site 2 is coupled to the right.

We chose many-body states for molecular subsystem in the form $|1\uparrow, 1\downarrow, 2\uparrow, 2\downarrow\rangle$. Unlike the choice of Refs. 42–45, these are not eigenstates of the molecular Hamiltonian. As a result the EOM for the Hubbard operator GFs couples them also by hopping $t_{12,\sigma}$. Besides this all the treatment presented in Sec. II remains the same. There are 16 states (1, 4, 6, 4, and 1 states for 0, 1, 2, 3, and 4 electrons in the system, respectively) and 32 single-electron transitions (16 for each spin block) to be considered.

Figure 4 shows the conductance map for elastic transport through a double quantum dot. The parameters of the calculation are $T=10$ K, $\varepsilon_{i\sigma}=-0.5$ eV, $t_{12,\sigma}=0.01$ eV, $\Gamma_{1\sigma}^L=\Gamma_{2\sigma}^R=0.01$ eV, $\Gamma_{1\sigma}^R=\Gamma_{2\sigma}^L=0$, $U_1=U_2=U=1$ eV, $U_{12}=0.5$ eV, and $E_F=0.5$ eV. As usual one sees pattern of blocked and allowed transport regions. However, here this pattern is more complicated than in the case of a single quantum dot. Figure 5 demonstrates this pattern for source-drain voltage $V_{sd}/U=0.25$. Shown are the current (a) and probabilities (b) of finding the molecular subsystem in different occupation states.

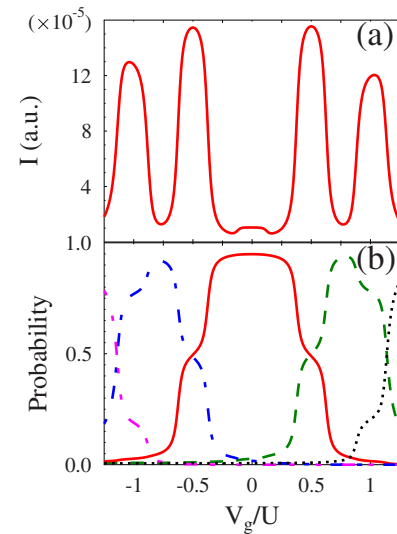


FIG. 5. (Color online) Elastic transport through a double quantum dot at fixed source-drain voltage $V_{sd}/U=0.25$: (a) current vs gate voltage and (b) probability of finding a double quantum dot empty (dotted line, black), singly (dashed line, green), doubly (solid line, red), triply (dash-dotted line, blue), or fully occupied (dash-double-dotted line, magenta). Parameters are the same as in Fig. 4.

IV. CONCLUSION

Approaches based on renormalization-group technique [numerical renormalization group (NRG), density matrix renormalization group (DMRG), real time renormalization group, etc.] are routinely used to treat quantum impurity systems, where, e.g., correlations between localized impurity (quantum dot or molecule) and delocalized states (contacts) lead to the Kondo effect. Mostly these approaches were applied to description of strongly correlated systems in equilibrium. The description of transport is more problematic, since one needs to know the spectral function at finite temperature, where all excitations may contribute.⁵⁶ Nevertheless first approaches dealing with transport started to appear as well.^{36,56–60} The main complication with the implementation of these methods (besides DMRG) for *ab initio* calculation is their complexity, so that all the calculations done so far are restricted to simple models only. In the case of molecular junctions, most of *ab initio* calculations done today are performed at the mean-field level of treatment with effective single-particle orbitals used in place of molecular states. Such approach clearly breaks down in the resonance tunneling regime, where actual reduction/oxidation of the molecule leading to corresponding electronic and vibrational structure change becomes possible. The necessity of treating this regime in the language of many-body molecular states, thus incorporating on-the-molecule correlations, was realized, and first approaches such as, e.g., the generalized master-equation approach,^{25,26} were proposed. Here we generalize this consideration by incorporating many-body molecular states language into the nonequilibrium Green's-function framework. The main formal problem here is that many-body state language makes the Wick theorem inapplicable; thus standard nonequilibrium diagrammatic techniques cannot be used. A workaround based on the functional derivative

equation-of-motion technique for the Hubbard operator GFs was developed by Sandalov *et al.*³⁸ for the equilibrium case. The method so far has been applied in modeling elastic transport through quantum dots^{39–41} and the lowest states of double quantum dots,^{42–45} and is completely ignored in the molecular electronics community. Here we employ the approach in dealing with inelastic transport through molecular junctions in a nonequilibrium atomic limit. We formulate the method within the basis of the charged states of the molecule. We demonstrate its ability to deal with the transport situation in the language of these states (rather than effective single-electron orbitals), as well as to take into account charge-specific normal modes and nonadiabatic couplings. The capabilities of the technique are illustrated with simple model calculations of transport through a quantum dot and a double quantum dot. Extension to realistic calculations is the goal of our future research.

ACKNOWLEDGMENTS

M.G. is indebted to Igor Sandalov for numerous illuminating discussions, and thanks Karsten Flensberg, Jonas Fransson, and Ivar Martin for helpful conversations. M.G. gratefully acknowledges support from the UCSD Startup Fund and the LANL. A.N. thanks the Israel Science Foundation, the U.S.-Israel Binational Science Foundation, and the German-Israel Foundation for financial support. M.A.R. thanks the NSF/MRSEC for support, through the NU-MRSEC. This work was performed in part at the Center for Integrated Nanotechnologies, a U.S. Department of Energy, Office of Basic Energy Sciences user facility. The Los Alamos National Laboratory is operated by Los Alamos National Security, LLC for the National Nuclear Security Administration of the U.S. Department of Energy under Contract No. DE-AC52-06NA25396.

*Also at Theoretical Division and Center for Integrated Nanotechnologies, Los Alamos National Laboratory, Los Alamos, NM 87545, USA.

¹A. Nitzan and M. A. Ratner, *Science* **300**, 1384 (2003).

²R. Landauer, *IBM J. Res. Dev.* **1**, 223 (1957).

³B. C. Stipe, M. A. Rezaei, and W. Ho, *Phys. Rev. Lett.* **82**, 1724 (1999).

⁴N. B. Zhitenev, H. Meng, and Z. Bao, *Phys. Rev. Lett.* **88**, 226801 (2002).

⁵M. Galperin, M. A. Ratner, and A. Nitzan, *J. Phys.: Condens. Matter* **19**, 103201 (2007).

⁶M. Galperin, M. A. Ratner, A. Nitzan, and A. Troisi, *Science* **319**, 1056 (2008).

⁷R. Lake and S. Datta, *Phys. Rev. B* **45**, 6670 (1992).

⁸R. Lake and S. Datta, *Phys. Rev. B* **46**, 4757 (1992).

⁹S. Tikhodeev, M. Natario, K. Makoshi, T. Mii, and H. Ueba, *Surf. Sci.* **493**, 63 (2001).

¹⁰T. Mii, S. Tikhodeev, and H. Ueba, *Surf. Sci.* **502-503**, 26 (2002).

¹¹T. Mii, S. G. Tikhodeev, and H. Ueba, *Phys. Rev. B* **68**, 205406

(2003).

¹²M. Galperin, M. A. Ratner, and A. Nitzan, *J. Chem. Phys.* **121**, 11965 (2004).

¹³N. Lorente, M. Persson, L.-J. Lauhon, and W. Ho, *Phys. Rev. Lett.* **86**, 2593 (2001).

¹⁴M.-L. Bocquet, H. Lesnard, and N. Lorente, *Phys. Rev. Lett.* **96**, 096101 (2006).

¹⁵T. Frederiksen, M. Brandbyge, N. Lorente, and A.-P. Jauho, *Phys. Rev. Lett.* **93**, 256601 (2004).

¹⁶M. Paulsson, T. Frederiksen, and M. Brandbyge, *Nano Lett.* **6**, 258 (2006).

¹⁷N. Lorente and M. Persson, *Phys. Rev. Lett.* **85**, 2997 (2000).

¹⁸A. Pecchia, A. Di Carlo, A. Gagliardi, S. Sanna, T. Frauenheim, and R. Gutierrez, *Nano Lett.* **4**, 2109 (2004).

¹⁹P. Hyldgaard, S. Hershfield, J. H. Davies, and J. W. Wilkins, *Ann. Phys. (N.Y.)* **236**, 1 (1994).

²⁰A. Mitra, I. Aleiner, and A. J. Millis, *Phys. Rev. B* **69**, 245302 (2004).

²¹N. S. Wingreen, K. W. Jacobsen, and J. W. Wilkins, *Phys. Rev. Lett.* **61**, 1396 (1988).

- ²²N. S. Wingreen, K. W. Jacobsen, and J. W. Wilkins, *Phys. Rev. B* **40**, 11834 (1989).
- ²³J. Bonča and S. A. Trugman, *Phys. Rev. Lett.* **75**, 2566 (1995).
- ²⁴A. S. Alexandrov and A. M. Bratkovsky, *Phys. Rev. B* **67**, 235312 (2003).
- ²⁵B. Muralidharan, A. W. Ghosh, and S. Datta, *Phys. Rev. B* **73**, 155410 (2006).
- ²⁶L. Siddiqui, A. W. Ghosh, and S. Datta, *Phys. Rev. B* **76**, 085433 (2007).
- ²⁷K. Flensberg, *Phys. Rev. B* **68**, 205323 (2003).
- ²⁸M. Galperin, A. Nitzan, and M. A. Ratner, *Phys. Rev. B* **73**, 045314 (2006).
- ²⁹R. Härtle, C. Benesch, and M. Thoss, *Phys. Rev. B* **77**, 205314 (2008).
- ³⁰M. Galperin, M. A. Ratner, and A. Nitzan, *Nano Lett.* **5**, 125 (2005); M. Galperin, A. Nitzan, and M. A. Ratner, *J. Phys.: Condens. Matter* **20**, 374107 (2008).
- ³¹A. La Magna and I. Deretzis, *Phys. Rev. Lett.* **99**, 136404 (2007).
- ³²A. M. Kuznetsov, *J. Chem. Phys.* **127**, 084710 (2007).
- ³³A. Mitra, I. Aleiner, and A. J. Millis, *Phys. Rev. Lett.* **94**, 076404 (2005).
- ³⁴D. Mozyrsky, M. B. Hastings, and I. Martin, *Phys. Rev. B* **73**, 035104 (2006).
- ³⁵J. P. Bergfield and C. A. Stafford, arXiv:0803.2756 (unpublished).
- ³⁶H. Schoeller, *Lect. Notes Phys.* **544**, 137 (2000).
- ³⁷J. Rammer, A. L. Shelankov, and J. Wabnig, *Phys. Rev. B* **70**, 115327 (2004).
- ³⁸I. Sandalov, J. Johansson, and O. Eriksson, *Int. J. Quantum Chem.* **94**, 113 (2003).
- ³⁹J. Fransson, O. Eriksson, and I. Sandalov, *Phys. Rev. Lett.* **88**, 226601 (2002).
- ⁴⁰J. Fransson, *Phys. Rev. B* **72**, 075314 (2005).
- ⁴¹I. Sandalov and R. G. Nazmitdinov, *Phys. Rev. B* **75**, 075315 (2007).
- ⁴²J. Fransson, O. Eriksson, and I. Sandalov, *Photonics Nanostruct. Fundam. Appl.* **2**, 11 (2004).
- ⁴³J. Fransson and O. Eriksson, *J. Phys.: Condens. Matter* **16**, L85 (2004).
- ⁴⁴J. Fransson, *Phys. Rev. B* **69**, 201304(R) (2004).
- ⁴⁵J. Fransson and O. Eriksson, *Phys. Rev. B* **70**, 085301 (2004).
- ⁴⁶M. Galperin, A. Nitzan, and M. A. Ratner, *Phys. Rev. B* **74**, 075326 (2006).
- ⁴⁷T. S. Rahman, R. S. Knox, and V. M. Kenkre, *Chem. Phys.* **44**, 197 (1979).
- ⁴⁸J. Fransson, O. Eriksson, and I. Sandalov, *Phys. Rev. B* **66**, 195319 (2002).
- ⁴⁹Y. Meir and N. S. Wingreen, *Phys. Rev. Lett.* **68**, 2512 (1992).
- ⁵⁰H. Haug and A. Jauho, *Quantum Kinetics in Transport and Optics of Semiconductors* (Springer-Verlag, Berlin, 1996).
- ⁵¹Note that an approximation such as the one presented in Sec. II D may result in unphysical behavior. In particular, retarded and advanced SEs and GFs are not Hermitian conjugates of one another. While the issue does not arise in the diagonal approximation implemented for calculations here, this is a problem for a more general consideration. A simple workaround is to use the average of two Dyson-type expressions: one with \hat{D}^{-1} [Eq. (35)] applied from the left and one with \hat{D}^{-1} applied from the right. This leads to a set of equations for GFs, which under Markov approximation are reduced to widely employed equations for density matrix (DM) in dissipative environment.
- ⁵²M. Galperin, A. Nitzan, and M. A. Ratner, *Phys. Rev. B* **76**, 035301 (2007).
- ⁵³G. D. Mahan, *Many-Particle Physics* (Kluwer Academic, Dordrecht/Plenum, New York, 2000).
- ⁵⁴P. T. Ruhoff, *Chem. Phys.* **186**, 355 (1994).
- ⁵⁵P. T. Ruhoff and M. A. Ratner, *Int. J. Quantum Chem.* **77**, 383 (2000).
- ⁵⁶R. Bulla, T. A. Costi, and T. Pruschke, *Rev. Mod. Phys.* **80**, 395 (2008).
- ⁵⁷K. A. Al-Hassanieh, A. E. Feiguin, J. A. Riera, C. A. Busser, and E. Dagotto, *Phys. Rev. B* **73**, 195304 (2006).
- ⁵⁸J. E. Han, *Phys. Rev. B* **73**, 125319 (2006).
- ⁵⁹P. S. Cornaglia, G. Usaj, and C. A. Balseiro, *Phys. Rev. B* **76**, 241403(R) (2007).
- ⁶⁰F. B. Anders, *Phys. Rev. Lett.* **101**, 066804 (2008).